Theoretical Notes
Note 168

SC-RR-71 0870

FIELD GENERATION WITHIN A LOSSY DIELECTRIC CYLINDER EXCITED BY A RADIATION PULSE

D. L. Mangan
G. J. Scrivner
Radiation Effects Division II
Sandia Laboratories, Albuquerque, New Mexico
87115

February 1972

ABSTRACT

A transient electromagnetic field problem is solved for a finite length cylindrical cavity bounded by perfectly conducting walls. The cavity is filled with a homogeneous lossy dielectric material. Analytic solutions for the relevant components of the electric and magnetic fields generated by an axially propagating current pulse are presented. Results obtained for various sample problems are discussed.

Key words: electromagnetic fields, radiation effects

TABLE OF CONTENTS

LIST OF FIGURES

LIST OF FIGURES
(continued)

FIELD GENERATION WITHIN A LOSSY DIELECTRIC CYLINDER EXCITED BY A RADIATION PULSE

INTRODUCTION

The interaction of gamma radiation with matter acts as a source of a spatially distributed electron current.[1] This current and its associated charge density result in the generation of electromagnetic fields. An understanding of both the magnitudes and the temporal behavior of these fields is required to interpret correctly some of the experimental observations pertinent to gamma radiation exposures from reactors, electron beam machines, and Nevada Test Site (NTS) devices. In addition, this knowledge would be useful in the design of instrumentation and electromagnetic sensitive devices which must perform reliably in such environments.

The electromagnetic fields existing in some bounded region can be associated with the presence of charge densities and currents both within and external to the region. In many practical situations, extensive effort is taken to provide a region isolated from the influence of sources external to it. We define such an idealized region as an electromagnetic cavity. At present we are restricting our investigations to the fields within such cavities and hence are only examining the effects of internally generated currents and charge densities.

Our present effort has been directed toward acquiring an exact analytical description of the fields associated with a simple model problem. In this paper we outline the derivation, present the general analytical solution, and examine several sample problems. We hope our results will provide insight into the response to be expected in various gamma environments of current interest.

DESCRIPTION OF THE MODEL PROBLEM

The physical configuration which we examine is a finite length cylindrical cavity having perfectly conducting boundaries and filled with a rather arbitrary medium. We assume that the radiation is incident on one of the end faces and results

[1] C. E. Baum, Unsaturated Compton Current and Space-Charge Fields in Evacuated Cavities, AFWL EMP 2-1, Air Force Weapons Laboratory, KAFB, New Mexico, April 1967.

only in an axially driven current. We assume no spatial variation of the induced current pulse in a plane perpendicular to the axis of the cylinder. Along the axis of the cylinder we assume that the current intensity is exponentially attenuated. With regard to the temporal behavior of this driving current, we take zero time to coincide with the instant that the radiation pulse impinges upon the front face of the cylinder. The temporal behavior of the current pulse is assumed to be identical throughout the cavity except for a simple time lag resulting from the axial propagation of the driving radiation pulse. We assume that the medium within the cavity is homogeneous and can be characterized by a time independent conductivity, permittivity, permeability, and linear attenuation coefficient. The geometry is shown in Fig. 1.

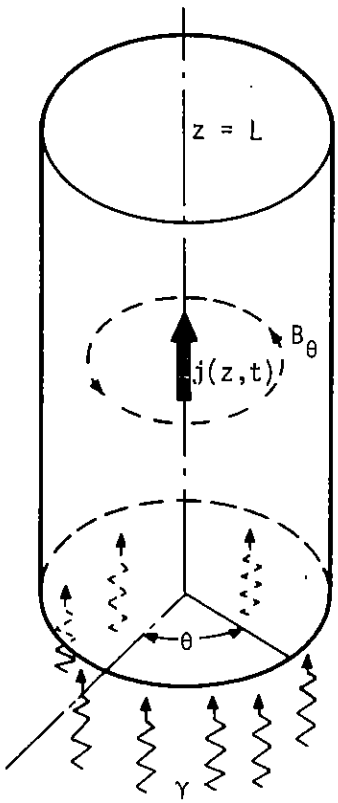

Fig. 1

Coordinate system for model.

MATHEMATICAL ANALYSIS

In this section we outline the flow of mathematical logic necessary to achieve the expressions for the electromagnetic response of the above stated problem. We will consistently employ the MKS system of units for which the appropriate forms of Maxwell's field equations are

$$\nabla \cdot \vec{D} = \rho \ , \tag{1}$$

$$\nabla \cdot \vec{B} = 0 \ , \tag{2}$$

$$\nabla \times \vec{E} = - \frac{\partial \vec{B}}{\partial t} \ , \tag{3}$$

and

$$\nabla \times \vec{H} = \vec{j} + \frac{\partial \vec{D}}{\partial t} + \sigma \vec{E}, \tag{4}$$

where σ is the medium conductivity, $\vec{j}$ is the radiation-produced current density, and ρ is its associated charge density. In addition, we have the constitutive equations which relate the electric displacement $\vec{D}$ to the electric field $\vec{E}$, and the magnetic field $\vec{B}$ to the magnetic field intensity $\vec{H}$:

$$\vec{D} = \varepsilon \vec{E} \tag{5}$$

and

$$\vec{B} = \mu \vec{H} \ , \tag{6}$$

where ε and μ are the medium permittivity and permeability, respectively. By operating with the curl on Eq. (3), one can obtain the following wave equation for the electric field $\vec{E}$:

$$\nabla^2 \vec{E} - \frac{1}{c^2}\left(\frac{\partial^2}{\partial t^2} + \frac{\sigma}{\varepsilon} \frac{\partial}{\partial t}\right)\vec{E} = \mu \frac{\partial \vec{j}}{\partial t} + \frac{1}{\varepsilon} \nabla \rho \ , \tag{7}$$

where c is the electromagnetic propagation velocity, $c^2 = 1/\mu\varepsilon$.

With $\vec{a}_z$ defined as the unit vector in the axial direction, the current density $\vec{j}$ is assumed to be expressible as

$$\vec{j} = j_o\left(t - \frac{z}{c}\right)e^{-\Sigma z}\vec{a}_z \ , \tag{8}$$

where Σ is the linear attenuation coefficient of the material within the cavity with respect to the incident radiation and where $j_o(t)$ describes the temporal behavior of the radiation pulse at the front face of the cavity, $z = 0$.

We use the following definition of the Laplace transform of a function F(t):

$$f(s) = \int_0^\infty F(t)e^{-st}\,dt\ . \tag{9}$$

Applying this transformation to Eqs. (7) and (8), and assuming that all fields are initially zero, we obtain

$$\nabla^2\vec{E} - \frac{1}{c^2}\left(s^2 + \frac{\sigma}{\varepsilon}\,s\right)\vec{E} = \mu s\vec{j} + \frac{1}{\varepsilon}\,\nabla\rho\ , \tag{10}$$

$$\vec{j} = j_o\, e^{-\delta z}\vec{a}_z \tag{11}$$

where $\delta = \Sigma + s/c$, j_o is the Laplace transform of $j_o(t)$, and $\vec{E}$, $\vec{j}$, and ρ are now understood to represent transformed quantities. From Eqs. (1) and (4) the appropriate charge conservation equation, expressed in transform space, is

$$\nabla\cdot\vec{j} + \left(s + \frac{\sigma}{\varepsilon}\right)\rho = 0. \tag{12}$$

Equation (12) enables us to express the charge density ρ in terms of the radiation-produced current density j, and allows us to rewrite Eq. (10) as

$$\nabla^2\vec{E} - \frac{1}{c^2}\left(s^2 + \frac{s\sigma}{\varepsilon}\right)\vec{E} = \hat{\alpha}\, e^{-\delta z}\vec{a}_z\ , \tag{13}$$

where

$$\hat{\alpha} = j_o\,\frac{s\left(\mu\sigma - \frac{2\Sigma}{c}\right) - \Sigma^2}{\varepsilon s + \sigma}\ . \tag{14}$$

Referring again to Fig. 1, we assume symmetry with respect to the coordinate θ and note that, since the θ-component of the electric field E_θ must vanish at all points on the boundary of the cavity, and since the θ-component of Eq. (13) is homogeneous, E_θ remains zero throughout the cavity. The previous comments, in conjunction with Eq. (3), enable us to deduce that the only existent component of the magnetic field is B_θ.

In order to acquire the desired solution, we begin by examining the z-component of Eq. (13):

$$\nabla^2 E_z - k^2 E_z = \hat{\alpha} e^{-\delta z} , \tag{15}$$

where $k^2 = [s^2 + (s\sigma/\epsilon)]/c^2$. The homogeneous part of this equation must satisfy

$$\nabla^2 E_z^h - k^2 E_z^h = 0. \tag{16}$$

To be consistent with the boundary condition that E_z vanish at $r = R$ (R being the cavity radius) and to provide a bounded solution at $r = 0$, E_z^h is restricted to be of the form

$$E_z^h = \sum_{n=1}^{\infty} J_o\left(\frac{\alpha_n r}{R}\right)\left(D_1^n \cosh\beta_n z + D_2^n \sinh\beta_n z\right) , \tag{17}$$

where D_1^n and D_2^n are constants yet to be determined, and $(\alpha_n; n = 1,2,3,\ldots)$ is defined as the ordered set of ascending positive roots of the equation

$$J_o(x) = 0 , \tag{18}$$

where $J_o(x)$ is the ordinary Bessel function of the first kind and of zero-th order, and

$$\beta_n^2 = \left(\frac{\alpha_n}{R}\right)^2 + k^2 . \tag{19}$$

We successfully guess a particular solution of Eq. (15) of the form

$$E_z^p = g(r) e^{-\delta z} , \tag{20}$$

which leads us to the general solution of Eq. (15):

$$E_z = \frac{\hat{\alpha}}{\hat{k}^2}\left[1 - \frac{J_o(\hat{k}r)}{J_o(\hat{k}R)}\right] e^{-\delta z} + \sum_{n=1}^{\infty} J_o\left(\frac{\alpha_n r}{R}\right)\left(D_1^n \cosh\beta_n z + D_2^n \sinh\beta_n z\right) , \tag{21}$$

where

$$\hat{k}^2 = \delta^2 - k^2 \ . \tag{22}$$

From Eqs. (11) and (12) we obtain the expression for the charge density ρ:

$$\rho = \frac{\delta j_o e^{-\delta z}}{s + \sigma/\varepsilon} \ . \tag{23}$$

Combining Eqs. (1), (5), (21), and (23), and performing an integration over r, we obtain

$$E_r = -\frac{\hat{\alpha}}{\hat{k}^3}\,\delta e^{-\delta z}\,\frac{J_1(\hat{k}r)}{J_o(\hat{k}R)} - \sum_{n=1}^{\infty}\frac{R}{\alpha_n}\,J_1\left(\frac{\alpha_n r}{R}\right)\beta_n\left(D_1^n \sinh\beta_n z + D_2^n \cosh\beta_n z\right). \tag{24}$$

Employing the boundary conditions that E_r vanish at $z = 0$ and $z = L$ (L is the length of the cavity), we obtain expressions for D_1^n and D_2^n. Using the transformed equivalent of Eq. (3), we are able to obtain an expression for H_θ.

To summarize, at this stage we have obtained solutions for E_z, E_r, and H_θ in transformed space:

$$E_z(r,z,s) = \frac{-2j_o}{R\varepsilon}\sum_{n=1}^{\infty}\frac{J_o\left(\alpha_n r/R\right)}{J_1\left(\alpha_n\right)\left(\delta^2 - \beta_n^2\right)\left(s + \sigma/\varepsilon\right)}\left\{\frac{\left[s(2\Sigma/c - \mu\sigma) + \Sigma^2\right]e^{-\delta z}}{\left(\alpha_n/R\right)}\right.$$

$$\left. + \frac{\delta\left(\alpha_n/R\right)}{\beta_n \sinh\beta_n L}\left[e^{-\delta L}\cosh\beta_n z - \cosh\beta_n(L - z)\right]\right\} , \tag{25}$$

$$E_r(r,z,s) = \frac{2j_o}{R\varepsilon}\sum_{n=1}^{\infty}\frac{J_1\left(\alpha_n r/R\right)\delta}{J_1\left(\alpha_n\right)\left(s + \sigma/\varepsilon\right)\left(\delta^2 - \beta_n^2\right)}$$

$$\left\{-e^{-\delta z} + \frac{1}{\sinh\beta_n L}\left[e^{-\delta L}\sinh\beta_n z + \sinh\beta_n(L - z)\right]\right\} , \tag{26}$$

and

$$H_\theta(r,z,s) = \frac{-2j_o}{R}\sum_{n=1}^{\infty}\frac{J_1(\alpha_n r/R)}{J_1(\alpha_n)(\delta^2 - \beta_n^2)}\left\{e^{-\delta z}\right.$$

$$\left. + \frac{\delta}{\beta_n \sinh\beta_n L}\left[e^{-\delta L}\cosh\beta_n z - \cosh\beta_n(L - z)\right]\right\} . \qquad (27)$$

We now reconstruct the real time behavior of the electromagnetic response. We note that Eqs. (25), (26), and (27) are of the form

$$f(\vec{r},s) = j_o(s)\hat{f}(\vec{r},s) , \qquad (28)$$

where $\vec{r}$ denotes a position vector. The inversion of Eq. (28) is accomplished by recalling the Convolution theorem. Therefore, we write

$$F(\vec{r},t) = \int_0^t j_o(t - \tau)\hat{F}(\vec{r},\tau)\, d\tau , \qquad (29)$$

where $j_o(t) = \mathscr{L}^{-1}[j_o(s)]$, $\hat{F}(\vec{r},t) = \mathscr{L}^{-1}[\hat{f}(\vec{r},s)]$, and $\mathscr{L}^{-1}$ denotes the inverse Laplace transform operator. We use the Theory of Residues to obtain the respective $\mathscr{L}^{-1}[\hat{f}(\vec{r},s)]$ of Eqs. (25), (26), and (27). In presenting the resultant expressions in real time, we use nondimensionalized quantities, where $t \to tc/L$, $r \to r/R$, $z \to z/L$, $\sigma \to \sigma L/\varepsilon c$, $\Sigma \to \Sigma L$, and $\lambda = L/R$:

$$\varepsilon\hat{E}_z(\vec{r},t) = 2u(t - z)\lambda\sum_{n=1}^{\infty}\frac{J_o(\alpha_n r)e^{-\sigma t}(\Sigma - \sigma)}{J_1(\alpha_n)\left[(\Sigma - \sigma)^2 - (\lambda\alpha_n)^2\right]}\left\{\frac{(\Sigma - \sigma)e^{-(\Sigma-\sigma)z}}{\lambda\alpha_n}\right.$$

$$\left. + \left[\frac{e^{-(\Sigma-\sigma)}\cosh(\lambda\alpha_n z) - \cosh[\lambda\alpha_n(1 - z)]}{\sinh(\lambda\alpha_n)}\right]\right\}$$

$$+ 2u(t - z)\lambda\sum_{n=1}^{\infty}\frac{J_o(\alpha_n r)}{J_1(\alpha_n)}\lambda\alpha_n e^{-\sigma t/2}\sum_{m=0}^{\infty}\frac{\eta_m}{D_{mn}\left[(\sigma/2)^2 + \omega_{nm}^2\right]}$$

$$\left\{\left(\omega_{nm}A_{nm} - \frac{\sigma B_{nm}}{2}\right)\left[e^{-\hat{\Sigma}}\cos(m\pi z)\cos\left(\omega_{nm}(t - 1)\right) - \cos\left(m\pi(1 - z)\right)\cos\left(\omega_{nm}t\right)\right]\right.$$

$$-\left(\frac{\sigma A_{nm}}{2} + \omega_{nm}B_{nm}\right)\left[e^{-\hat{\Sigma}}\cos(m\pi z)\sin\left(\omega_{nm}(t-1)\right) - \cos\left(m\pi(1-z)\right)\sin\left(\omega_{nm}t\right)\right]\Bigg\}; \quad (30)$$

$$\varepsilon\hat{E}_r(\vec{r},t) = 2u(t-z)\lambda\sum_{n=1}^{\infty}\frac{J_1(\alpha_n r)(\Sigma-\sigma)e^{-\sigma t}}{J_1(\alpha_n)\left[(\Sigma-\sigma)^2 - (\lambda\alpha_n)^2\right]}\Bigg\{-e^{-(\Sigma-\sigma)z}$$

$$+\left[\frac{e^{-(\Sigma-\sigma)}\sinh(\lambda\alpha_n z) + \sinh\left[\lambda\alpha_n(1-z)\right]}{\sinh(\lambda\alpha_n)}\right]\Bigg\}$$

$$+ 2u(t-z)\lambda\sum_{n=1}^{\infty}\frac{J_1(\alpha_n r)}{J_1(\alpha_n)}e^{-\sigma t/2}\sum_{m=1}^{\infty}\frac{m\pi\eta_m}{D_{nm}\left[(\sigma/2)^2 + \omega_{nm}^2\right]}$$

$$\Bigg\{\left(\omega_{nm}A_{nm} - \frac{\sigma B_{nm}}{2}\right)\left[e^{-\hat{\Sigma}}\sin(m\pi z)\cos\left(\omega_{nm}(t-1)\right) + \sin\left(m\pi(1-z)\right)\cos\left(\omega_{nm}t\right)\right]$$

$$-\left(\frac{\sigma A_{nm}}{2} + \omega_{nm}B_{nm}\right)\left[e^{-\hat{\Sigma}}\sin(m\pi z)\sin\left(\omega_{nm}(t-1)\right) + \sin\left(m\pi(1-z)\right)\sin\left(\omega_{nm}t\right)\right]\Bigg\}; \quad (31)$$

$$\frac{\hat{H}_\theta(\vec{r},t)}{c} = -2u(t-z)\lambda\sum_{n=1}^{\infty}\frac{J_1(\alpha_n r)}{J_1(\alpha_n)}e^{-\sigma t/2}\sum_{m=0}^{\infty}\frac{\eta_m}{D_{nm}}$$

$$\Bigg\{A_{nm}\left[e^{-\hat{\Sigma}}\cos(m\pi z)\sin\left(\omega_{nm}(t-1)\right) - \cos\left(m\pi(1-z)\right)\sin\left(\omega_{nm}t\right)\right]$$

$$+ B_{nm}\left[e^{-\hat{\Sigma}}\cos(m\pi z)\cos\left(\omega_{nm}(t-1)\right) - \cos\left(m\pi(1-z)\right)\cos\left(\omega_{nm}t\right)\right]\Bigg\}; \quad (32)$$

where

$$\omega_{nm} = \left[(m\pi)^2 + (\lambda\alpha_n)^2 - \left(\frac{\sigma}{2}\right)^2\right]^{1/2}, \quad (33)$$

$$\hat{\Sigma} = \Sigma - \frac{\sigma}{2}, \quad (34)$$

$$A_{nm} = \hat{\Sigma}\left[\hat{\Sigma}^2 + (\omega_{nm})^2 + (m\pi)^2\right], \quad (35)$$

$$B_{nm} = \omega_{nm}\left[-\hat{\Sigma}^2 - (\omega_{nm})^2 + (m\pi)^2\right], \quad (36)$$

$$D_{nm} = \omega_{nm}\left\{\left[\hat{\Sigma}^2 - \left(\omega_{nm}\right)^2 + \left(m\pi\right)^2\right]^2 + 4\left(\omega_{nm}\hat{\Sigma}\right)^2\right\}, \tag{37}$$

$$\eta_m = \begin{cases} 1 \text{ if } m = 0 \\ 2(-1)^m \text{ if } m > 0 \end{cases}, \tag{38}$$

and

$$u(x) = \begin{cases} 0 \text{ if } x < 0 \\ 1 \text{ if } x > 0 \end{cases}. \tag{39}$$

Since the unit step is present in all of the above equations as a result of the fact that the fields at a distance z from the front face of the cavity are zero prior to the arrival of communication of the initial phase of excitation to that point, Eq. (29) can be equivalently expressed as

$$F(\vec{r},t) = \int_0^{t-z/c} j_o(\tau)\hat{F}(\vec{r},t-\tau)\, d\tau . \tag{40}$$

If one specifies $j_o(t)$, Eq. (40) can be applied to $\hat{E}_z$, $\hat{E}_r$, and $\hat{H}_\theta$ to obtain the desired electromagnetic response.

A few observations about the basic analytic structure of the resultant equations are appropriate. First, the inclusion of conductivity provides a method of energy dissipation resulting in both the expected damping of the electromagnetic response and the typical alteration of the characteristic response frequencies of the cavity. For large values of conductivity we note from Eq. (33) that ω_{nm} can become imaginary. Hence, for a relatively small conductivity, all the characteristic response modes of the cavity are underdamped. As the conductivity is increased, the response mode corresponding to the lowest characteristic frequency eventually becomes critically damped. Any additional increase in the conductivity results in an overdamped response of this mode. An identical conclusion is valid for higher response modes if the conductivity becomes sufficiently large. Second, the entire magnetic response function, $\hat{H}_\theta$, consists of a composite of damped sinusoidal temporal behavior indicative of the underlying wave nature of the magnetic field. The same observation is applicable to only a part of the expressions for the two components of the electric response functions, $\hat{E}_r$ and $\hat{E}_z$. Each of these latter two response functions contain an additional term which can be associated with the establishment of a charge density within the cavity. If the medium has finite conductivity, this term is exponentially damped

consistent with the characteristic relaxation of any established charge density within a conducting medium. It should be noted that this term only contributes to the solution if one has a nonzero conductivity and/or linear attenuation coefficient.

DISCUSSION OF SAMPLE PROBLEM RESULTS

The equations obtained in the previous section were programmed for the CDC 6600 computer. Our initial calculations have been restricted to an examination of a cylinder having a length-to-diameter ratio of 0.2. The time behavior of the radiation-produced current density pulse is taken to be

$$j_o(t) = -j_m \frac{t}{\alpha} \exp(1 - t/\alpha) \ , \tag{41}$$

where j_m is the maximum value of the current density which is attained when t equals α. Figure 2 is a normalized plot of Eq. (41). In the remaining graphs we depict the variation of the electromagnetic field behavior as a function of the pulse duration parameter α, the conductivity of the medium σ, and linear attenuation coefficient, Σ. The results are presented in nondimensionalized parameters.

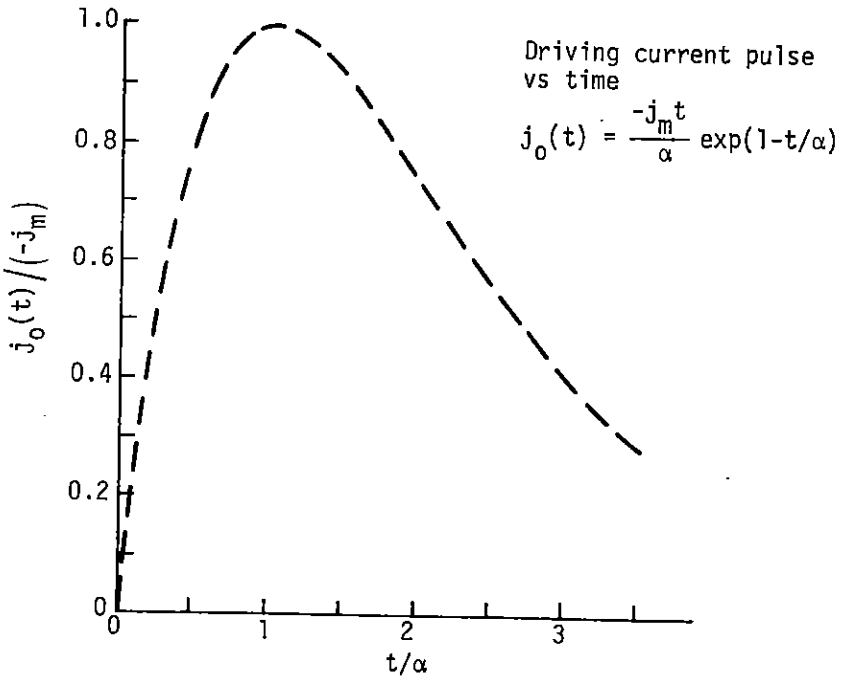

Fig. 2 Normalized plot of the driving current density temporal behavior.

Field Variation With α

The time behavior of the magnetic field at a specific point within the cavity is displayed in Fig. 3 for various values of the nondimensionalized pulse duration parameter $\alpha c/L$. Both σ and Σ are taken to be zero in these calculations. The lowest nondimensionalized resonant frequency of the cavity, $\omega_{1,0}L/c$, is 0.96. This characteristic frequency is quite apparent in the oscillatory behavior of the magnetic field for both pulse durations presented in Fig. 3. It is obvious from Fig. 3 that the intensity of the oscillatory response has been effectively reduced by increasing the duration parameter of the driving pulse. For even larger values of $\alpha c/L$ than considered in this graph, the above oscillatory behavior becomes hardly discernible. In this case, the temporal behavior of the magnetic field response follows that of the driving current density pulse. We do not present the two components of the electric field corresponding to Fig. 3. However, we wish to point out that our comment relative to the variation of the intensity of the oscillatory response with respect to the pulse duration parameter is consistent with the behavior of these electric field components.

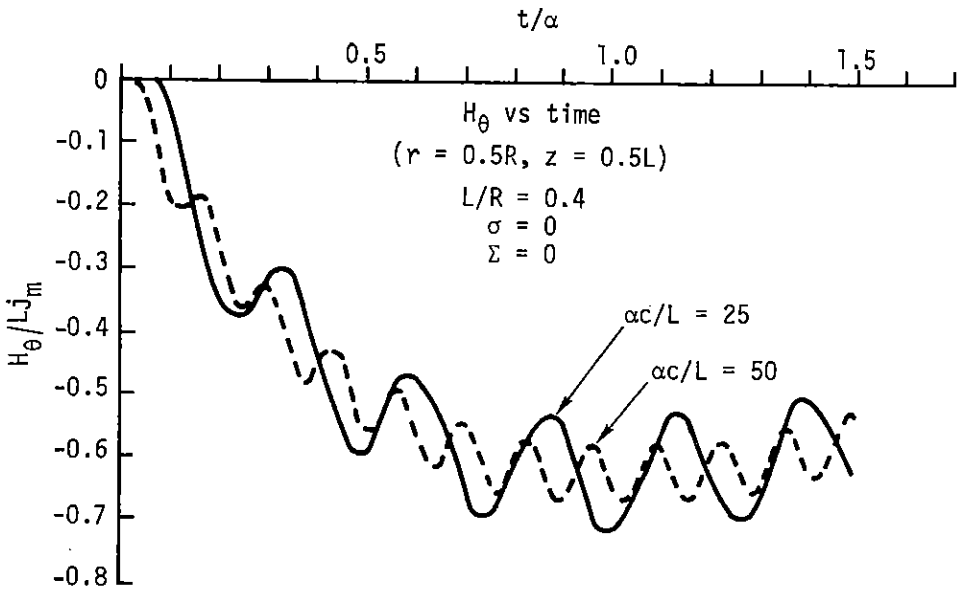

Fig. 3 Temporal behavior H_θ for various values of the driving pulse duration parameter $\alpha c/L$.

Field Variation With σ

In order to assess the influence of conductivity of the medium, we take Σ equal to zero and consider a pulse duration such that αc/L = 25. The time variation of the magnetic field at a specific point within the cavity is presented in Fig. 4 for three different values of conductivity. Although it is hardly noticeable from the curves, the effect of increasing the conductivity is a reduction in the frequency of the oscillatory behavior, as specified by Eq. (33), and a reduction in the effective driving current density due to the increased cancellation caused by the conduction process. More apparent is the damping of the oscillatory behavior for finite conductivity.

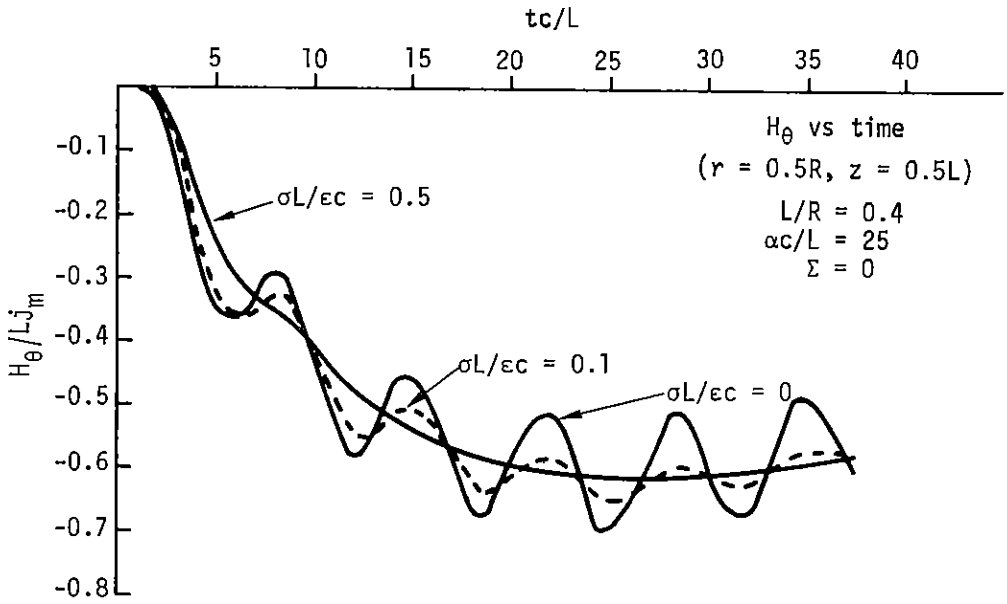

Fig. 4 Temporal behavior of H_θ for various values of the medium conductivity σL/(εc).

The corresponding behavior of the two components of the electric fields are summarized in Figs. 5 and 6.

Field Variation With Σ

We observe the effect of varying Σ by setting σ equal to zero and again choosing α equal to 25 L/c. The three field components are shown in Figs. 7 through 9. As can be noted from Fig. 7, the frequency of the time-varying magnetic field is insensitive to a change in Σ which is consistent with Eq. (33). As expected, the attenuation of the current density pulse affects a reduction in the magnitude of the magnetic response.

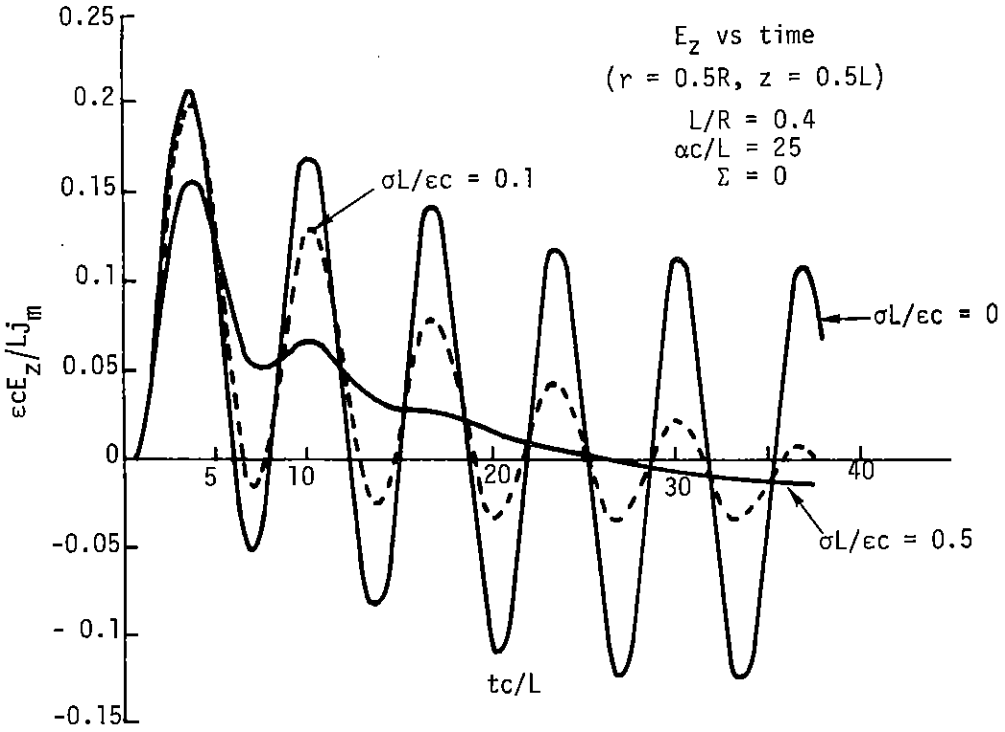

Fig. 5 Temporal behavior of E_z for various values of the medium conductivity $\sigma L/(\varepsilon c)$.

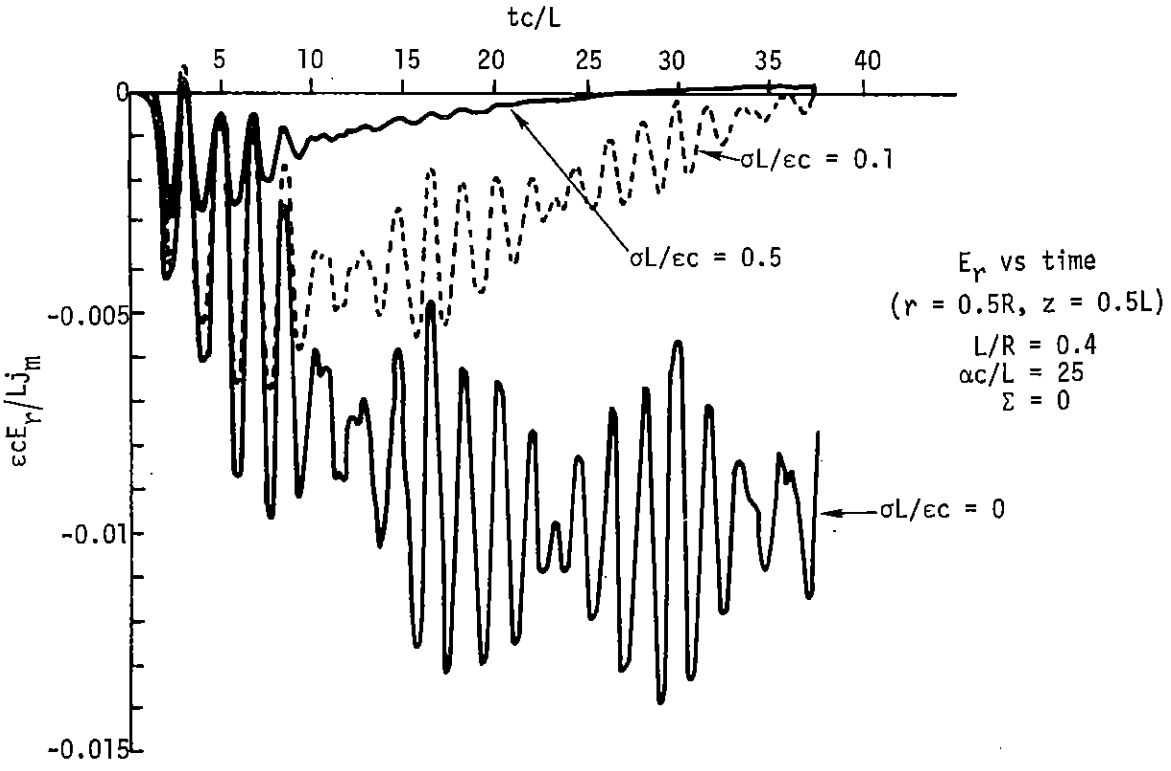

Fig. 6 Temporal behavior of E_r for various values of the medium conductivity $\sigma L/(\varepsilon c)$.

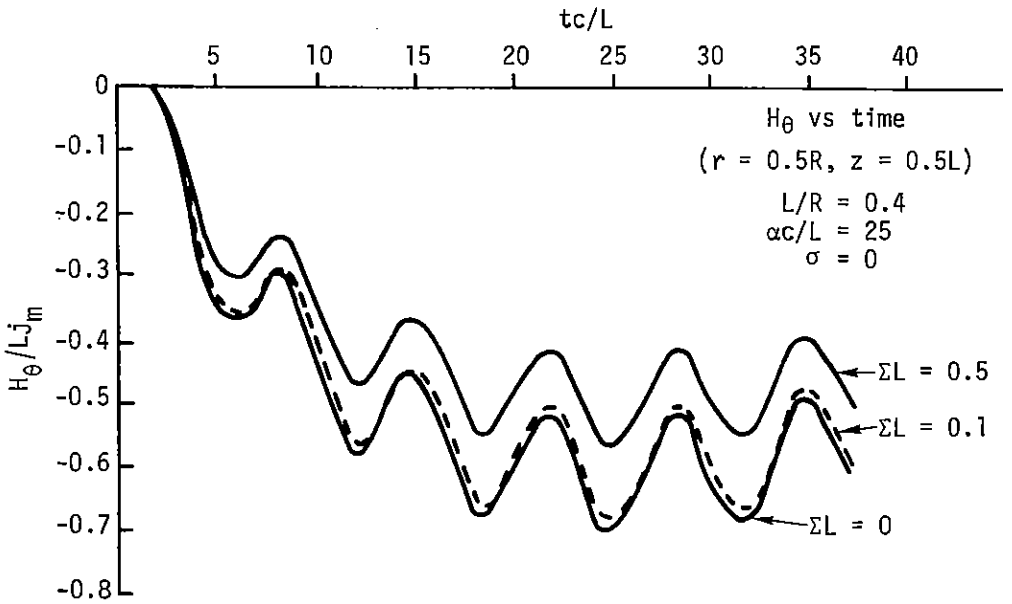

Fig. 7 Temporal behavior of H_θ for various values of the medium linear attenuation coefficient ΣL.

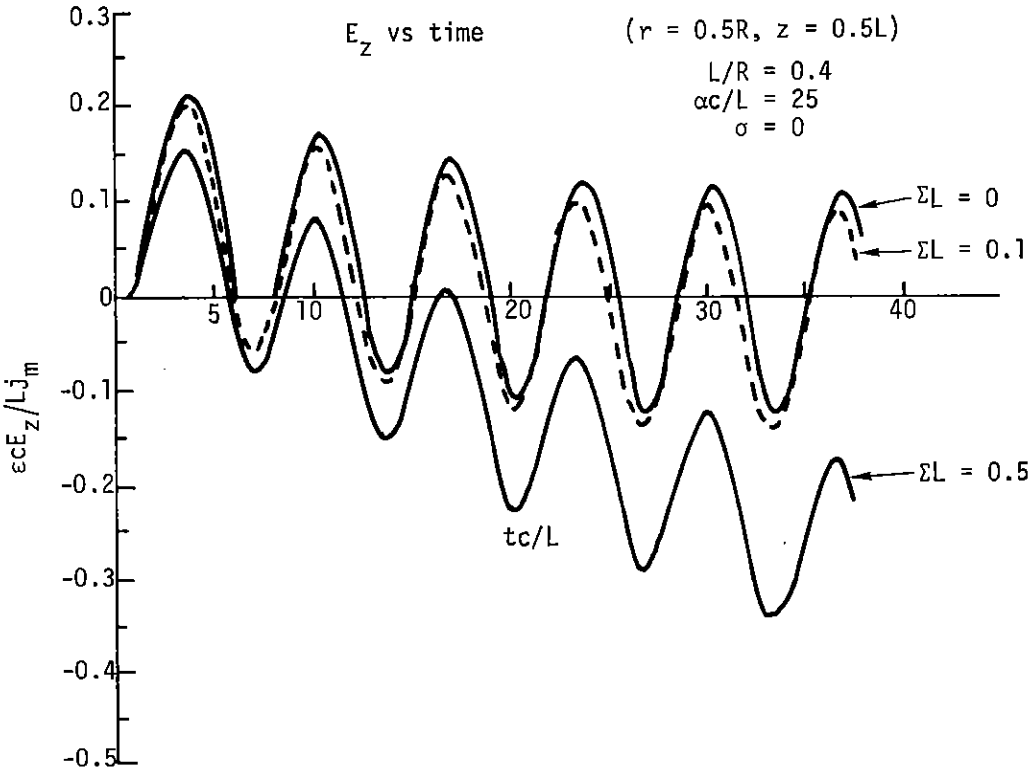

Fig. 8 Temporal behavior of E_z for various values of the medium linear attenuation coefficient ΣL.

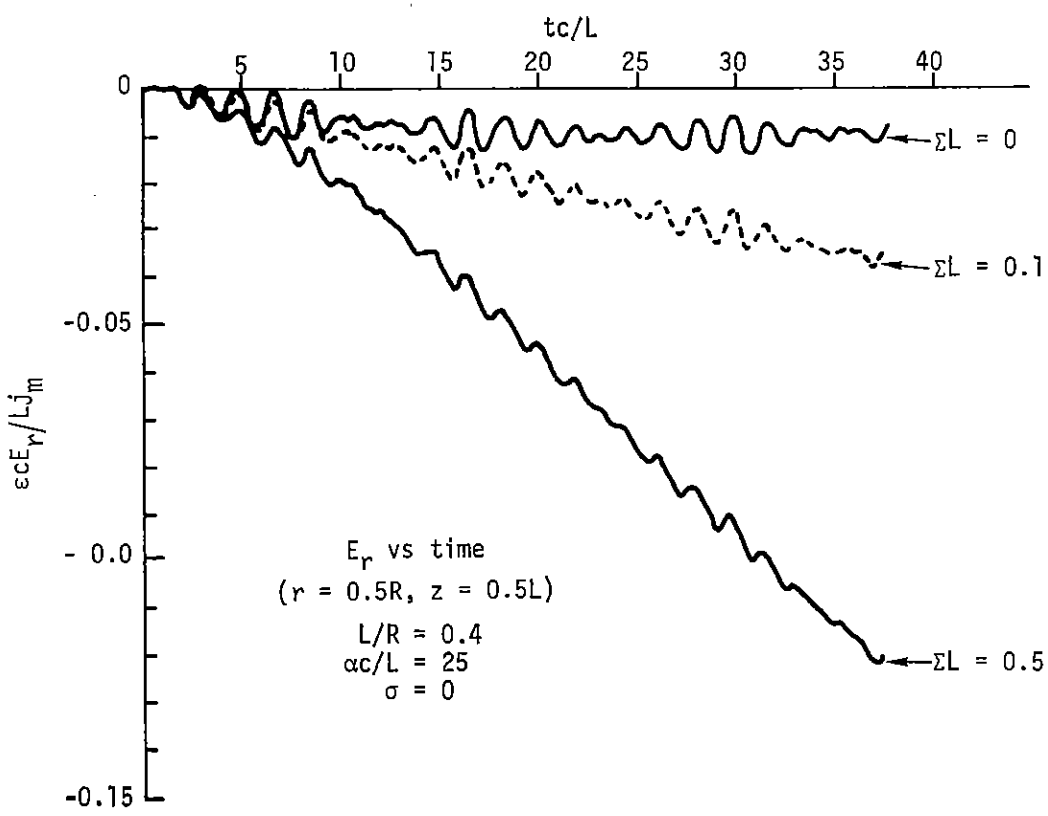

Fig. 9 Temporal behavior of E_r for various values of the medium linear attenuation coefficient ΣL.

In Figs. 8 and 9 both components of the electric field become negative as Σ is increased. This is caused by the buildup of a permanent charge density within the cavity. If this charge density were mobile, the electric field components are such that they would tend to diffuse the concentration of electrons near the front of the cylinder toward the rear and side walls of the cavity.

Spatial Dependence of the Electromagnetic Fields

To acquire insight into the spatial variation of the fields within the cavity, we consider the problem for which α equal 25 L/c and both σ and Σ are set equal to zero. Figure 10 shows the variation of the magnetic field with radial position for a specified axial position at various times. Except for the previously mentioned oscillatory behavior, the magnetic response can be estimated by ignoring the displacement current and solving the set of equations

$$\nabla \times \vec{H} = \vec{j}_o(t) \tag{42}$$

and

$$\nabla \cdot \vec{H} = 0. \tag{43}$$

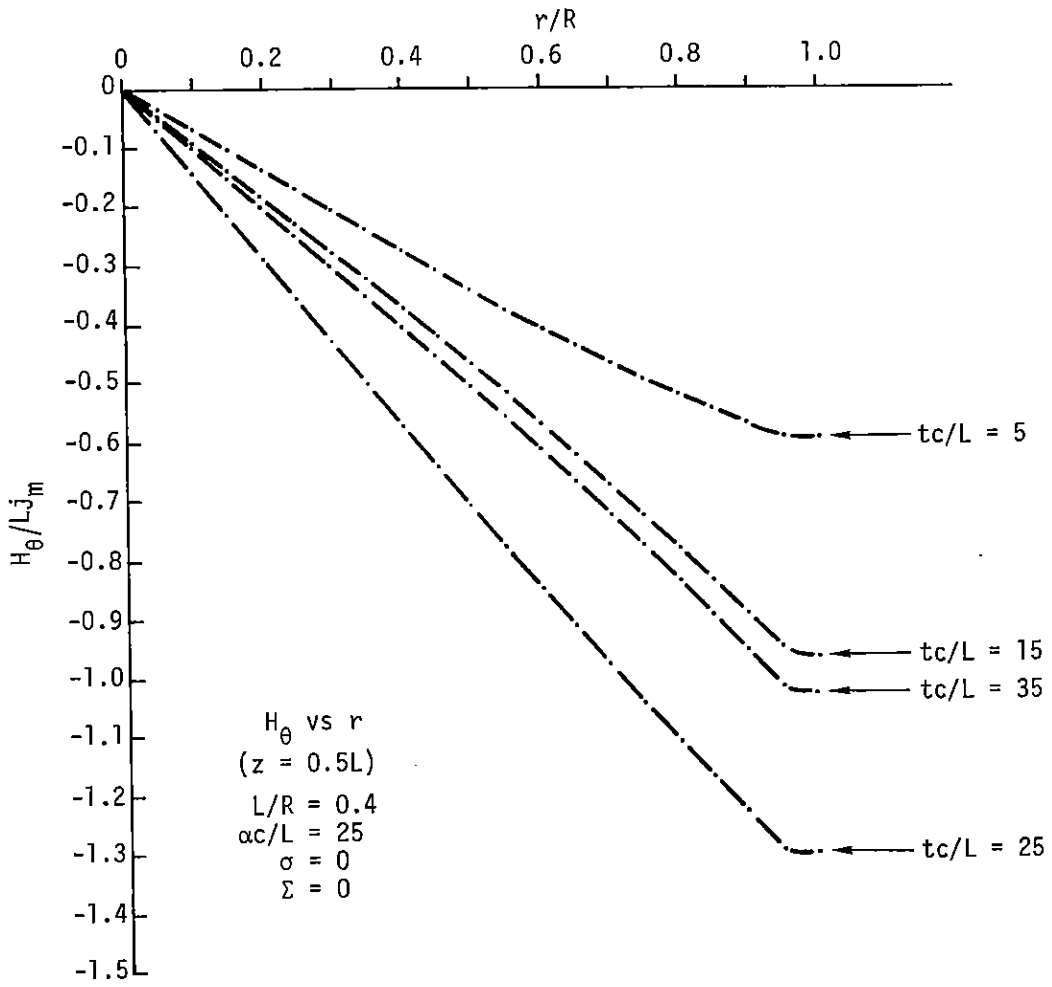

Fig. 10 radial variation of H_θ.

For the specific problem under investigation in this section, the above approximation would suggest a negligible variation in the magnetic field with respect to the z coordinate. This behavior is dramatically evident in Fig. 11.

The spatial variation in the two components of the electric field are shown in Figs. 12 through 15. Consistent with the boundary condition that the tangential component of the electric field vanish at the surface of a perfect conductor, we note

that E_z is zero at the side wall of the cavity, and E_r is zero at the front and back surfaces.

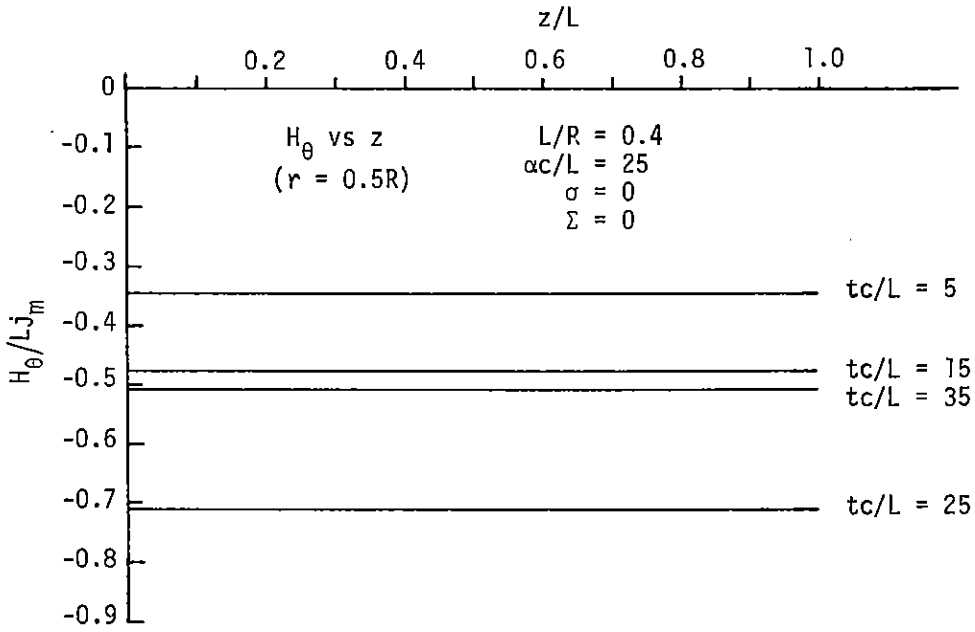

Fig. 11 Axial variation of H_θ.

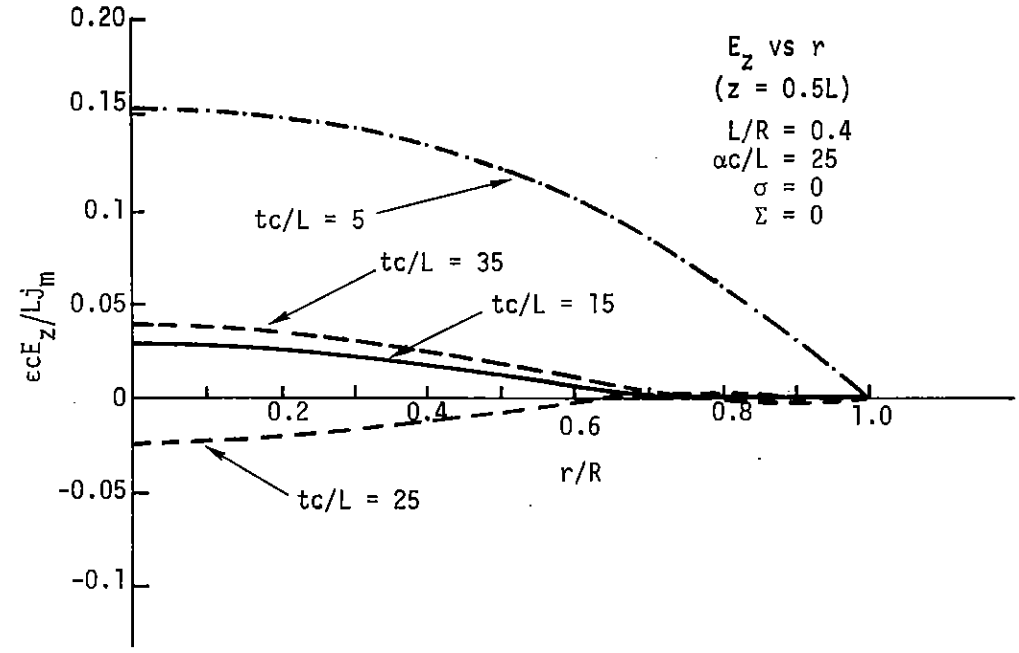

Fig. 12 Radial variation of E_z.

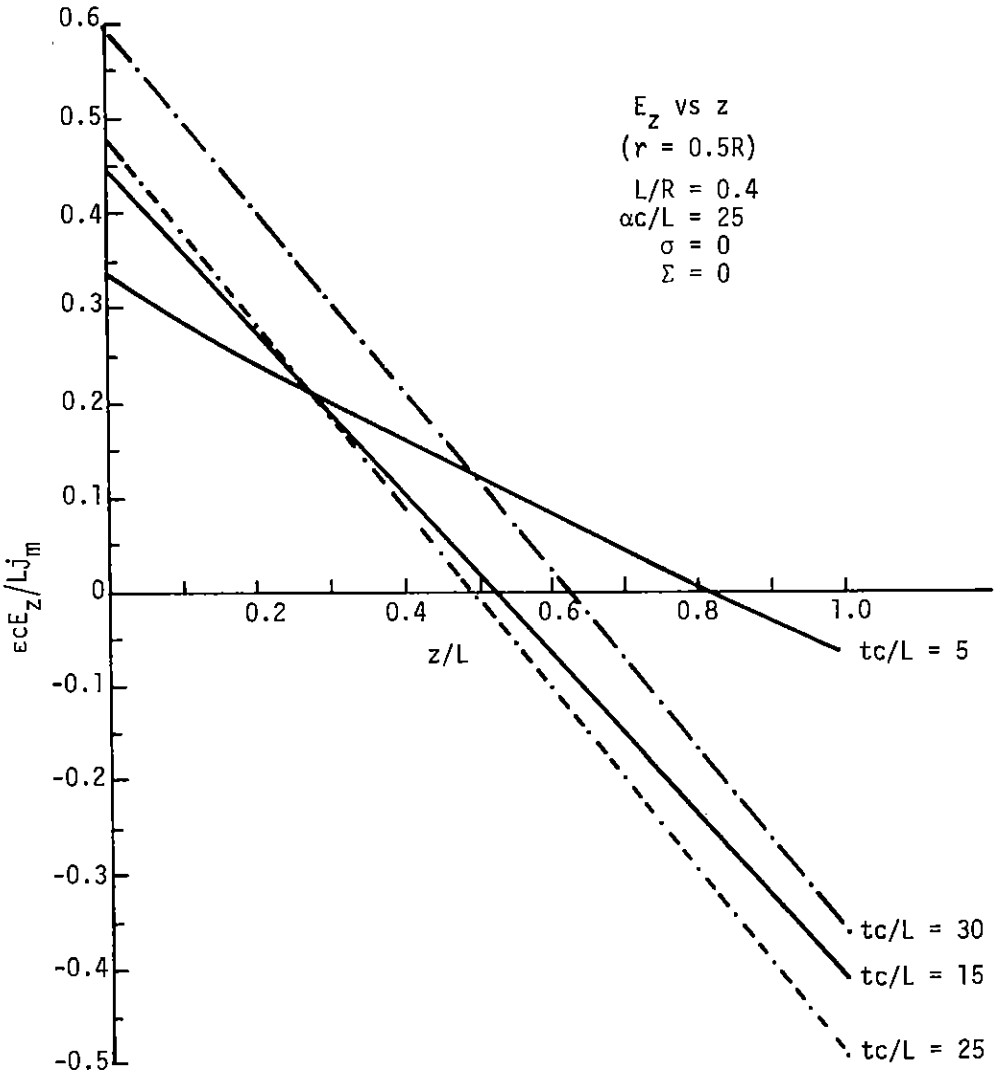

Fig. 13 Axial variation of E_z.

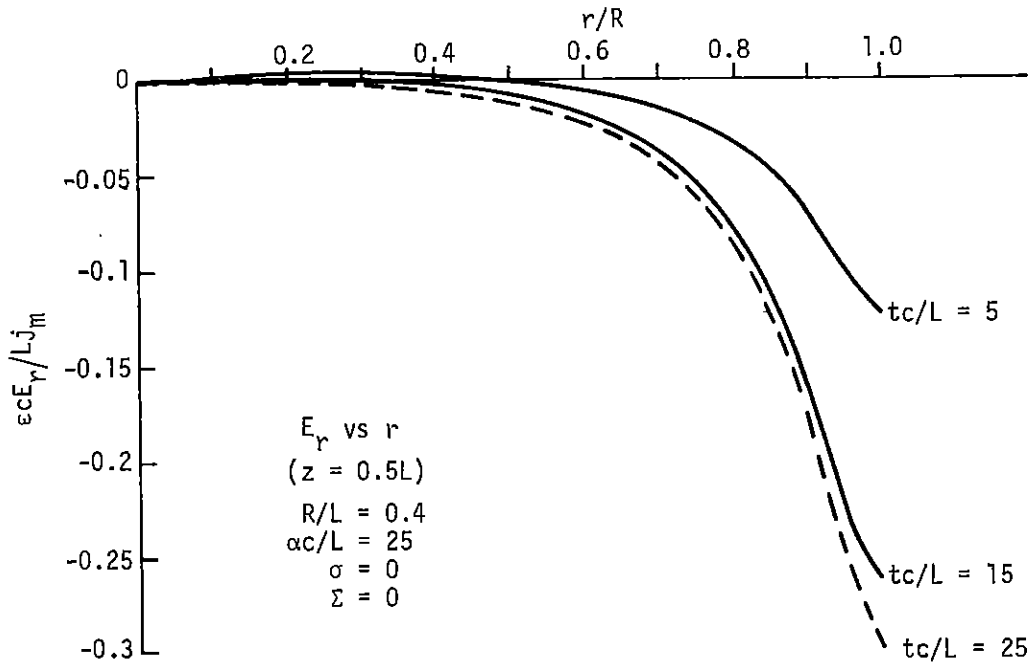

Fig. 14 Radial variation of E_r.

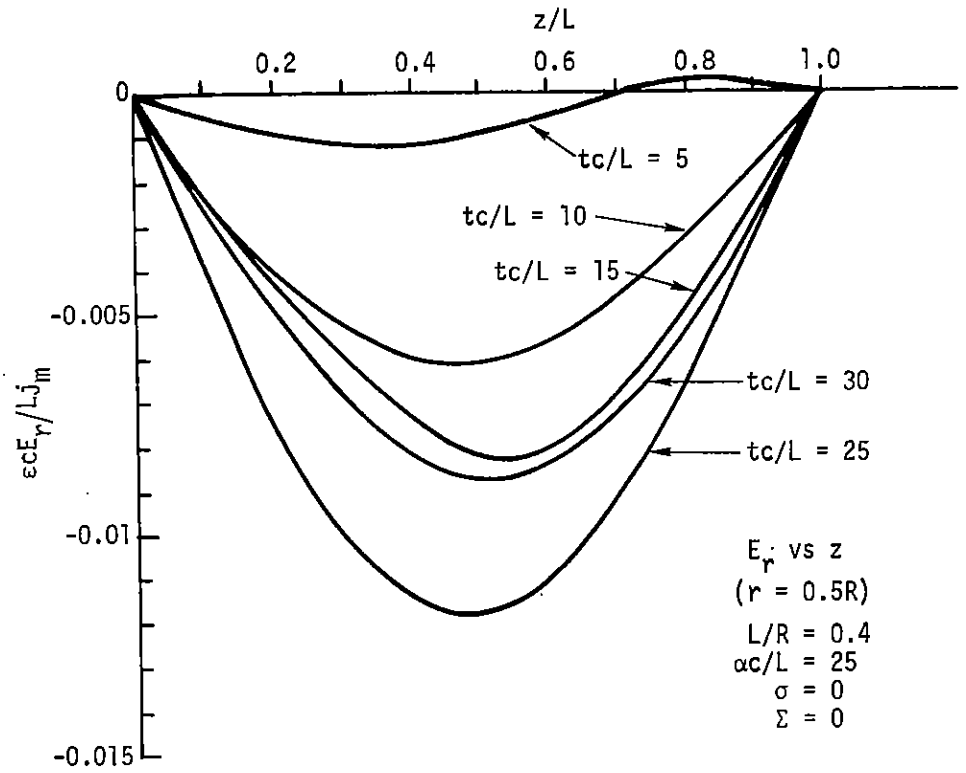

Fig. 15 Axial variation of E_r.

SUMMARY

We have outlined the mathematical method for obtaining the exact electromagnetic response of a cylindrical cavity excited by a radiation-driven current pulse. The computational results for a few specific cases of interest to us have been presented and discussed. Basically, the cavity responds as one would expect. Very little electromagnetic wave motion is established if the frequency content of the driving pulse is substantially lower than the resonant frequency of the cavity. The inclusion of conductivity provides a mechanism for energy dissipation which results in both a reduction in the frequency and a damping of the amplitudes associated with the oscillatory electromagnetic response. Including either a nonzero attenuation coefficient and/or a nonzero conductivity establishes a total current density gradient and a resultant charge density. This situation leads to the establishment of damped quasi-static electric field contributions. In addition, the driving current is effectively reduced, at least in a bulk sense, throughout the cavity, thereby reducing the amplitude of the magnetic response and the associated oscillatory electric response.

We have presented our solutions in the form of a double infinite sum. Equivalently, by ordering the eigen frequencies, a single summation could be accomplished. Regardless, such solutions are often of dubious computational value. It is fortunate that the degree of convergence of these expressions is adequate for meaningful computational results, at least for the subset of problems we have examined to date.

The analytic techniques utilized in this paper become grossly inadequate if one desires to treat more complex geometries and/or more complex physics. For more complex geometries, in most cases it will be impossible to choose a coordinate system which will permit the cavity boundaries to coincide with fixed coordinate surfaces. In addition, in such cases one no longer expects discrete response frequencies. If one desires to complicate the physics of this type of problem, by considering time-dependent electrical properties altered by the radiation pulse, or if the physics requires one to compensate for the interaction of the radiation-driven current with the induced electromagnetic fields, the linearity of the governing equations is destroyed. Any nonlinearity in the governing equations with respect to time makes application of conventional transform techniques impracticable. Such complex problems will require approximate and numerical methods to investigate electromagnetic response, and the solution of our model problem provides a limiting situation which should be useful for assessing the adequacy of such techniques as they are developed.